E201 244

(2)

PL-TR-91-2258

DATA DRIVEN IONOSPHERIC MAPPING TECHNIQUE FOR WIDE AREA NOWCASTING

Bodo W. Reinisch
Xueqin Huang
Gary S. Sales

University of Massachusetts, Lowell
Center for Atmospheric Research
450 Aiken Street
Lowell, Massachusetts 01854

September 1991

Scientific Report No. 4

PHILLIPS LABORATORY
Directorate of Geophysics
AIR FORCE SYSTEMS COMMAND
HANSCOM AIR FORCE BASE, MA 01731-5000

"This technical report has been reviewed and is approved for publication"

JURGEN BUCHAU
Contract Manager

JOHN E. RASMUSSEN
Branch Chief

FOR THE COMMANDER

WILLIAM K. VICKERY
Division Director

This report has been reviewed by the ESC Public Affairs Office (PA) and is releasable to the National Technical Information Service (NTIS).

Qualified requestors may obtain additional copies from the Defense Technical Information Center. All others should apply to the National Technical Information Service.

If your address has changed, or if you wish to be removed from the mailing list, or if the addressee is no longer employed by your organization, please notify PL/TSI, Hanscom AFB, MA 01731-5000. This will assist us in maintaining a current mailing list.

Do not return copies of this report unless contractual obligations or notices on a specific document requires that it be returned.

REPORT DOCUMENTATION PAGE

Form Approved
OMB No. 0704-0188

1. AGENCY USE ONLY (Leave blank)	2. REPORT DATE	3. REPORT TYPE AND DATES COVERED
	1991 September	Scientific Report No. 4

4. TITLE AND SUBTITLE
Data Driven Ionospheric Mapping Technique for Wide Area Nowcasting

5. FUNDING NUMBERS
PE 12417F
PR ESDO TA 01 WU AB
Contract:
F19628-90-K-0029

6. AUTHOR(S)
Bodo W. Reinisch
Xueqin Huang
Gary S. Sales

7. PERFORMING ORGANIZATION NAME(S) AND ADDRESS(ES)
University of Massachusetts Lowell
Center for Atmospheric Research
450 Aiken Street
Lowell, MA 01854

8. PERFORMING ORGANIZATION REPORT NUMBER

9. SPONSORING/MONITORING AGENCY NAME(S) AND ADDRESS(ES)
Phillips Laboratory
Hanscom AFB, MA 01731-5000

Contract Manager: Jurgen Buchau/LIS

10. SPONSORING/MONITORING AGENCY REPORT NUMBER
PL-TR-91-2258

11. SUPPLEMENTARY NOTES

12a. DISTRIBUTION/AVAILABILITY STATEMENT
Approved for public release;
Distribution unlimited

12b. DISTRIBUTION CODE

13. ABSTRACT *(Maximum 200 words)*

A new multidimensional mapping technique is being developed at the University of Massachusetts Lowell Center for Atmospheric Research, which determines the three dimensional electron density distribution of the ionosphere over a wide area of several thousand kilometers at any time, from sounder data recorded at the previous period just before this time. Electron density profiles from five Digisonde stations in the northeastern region of the North American continent are used to describe the electron distribution in a 30° longitude by 30° latitude region. The time histories over 32 hours of the profiles (the polynomial coefficients) from each station are Fourier transformed to determine the spectral components. For each spectral component a damped plane wave is fitted to amplitudes and phases at the five stations. This analysis is performed for each of the profile coefficients, and zonal maps are constructed as sums of these plane waves. This nowcasting technique can find applications in ray tracing for OTH radar, HF communicationand HF directon finding.

14. SUBJECT TERMS
Ionospheric mapping
Ionospheric models
Electron density profiles
Nowcasting

15. NUMBER OF PAGES
24

16. PRICE CODE

17. SECURITY CLASSIFICATION OF REPORT	18. SECURITY CLASSIFICATION OF THIS PAGE	19. SECURITY CLASSIFICATION OF ABSTRACT	20. LIMITATION OF ABSTRACT
Unclassified	Unclassified	Unclassified	SAR

TABLE OF CONTENTS

		Page
1.0	INTRODUCTION	1
2.0	PHYSICAL AND MATHEMATICAL FOUNDATION	3
3.0	DETERMINATION OF THE FOURIER KERNEL	5
4.0	APPLICATION OVER THE NORTHEASTERN AMERICAN COAST	7
5.0	EVALUATION OF THE NOWCASTING TECHNIQUE	14
6.0	SUMMARY	18
7.0	REFERENCES	19

LIST OF FIGURES

Figure No.		Page
1	Five Digisonde stations in the northeast American coastal region (G-Goose Bay, A-Argentia, M-Millstone Hill, W-Wallops Island and B-Bermuda) make routine half-hourly ionograms	8
2	Time-variation of parameter foF2 for 5 stations. To calculate the contour map for foF2 at 1300 UT on day 349, the previous 32 hours of data for each station are Fourier transformed. The data samples used for constructing the 1300 UT map are marked by small dots.	10
3	Spectra for parameter foF2 for 5 stations day 349, 1990, 13 UT The amplitude spectra determine which "wave frequencies" contribute to the parameter map. The amplitude and phase distribution for each spectrum component over the five stations specifies the attenuation and phase constants and the wave directions. Linear superposition of the set of plane waves generates the parameter contour map for the 30° by 30° area. Once the contour maps for all parameters are specified, the electron density profile at any point in the area is given by equation (3)	11
4	Sunrise sequence of foF2 maps. Systematic change of the foF2 contours as a function of time; half-hourly increments	12
5	Sunrise sequence of profile cross sections. Profile cross sections in any direction can be calculated through the mapped area. The time sequence of the east-west cross section during sunrise on day 349 in half-hour increments is shown	15
6	Evaluation of the mapping technique using the IRI database. RMS errors for foF2 and hmF2 at the 5 sounder sites and 16 other locations for January and July under low (R=10) and high (R=150) solar activity, respectively	17

1.0 INTRODUCTION

Ionospheric electron density distributions show great longitudinal and latitudinal variations in space, as well as diurnal, seasonal and solar cycle variations in time, even for the quiet ionosphere. Generally, ionospheric variations appear in a wave-like form with the wavelengths ranging from meters to several thousand kilometers. The electron density of the ionosphere is a function of the location coordinates X and Y, the altitude z, and the time t:

$$N = N(X,Y,z,t) \tag{1}$$

The task of ionospheric mapping is to find the function (1) as the best fit to the observed data from the sounding stations. Since the Digisonde network/1/ produces electron density profiles in real time, the potential exists to generate electron density maps in real time for areas with adequately located Digisondes. This paper describes the new three-dimensional mapping technique and shows preliminary results. After introducing the physical and mathematical foundation, the paper applies the technique to the Northeastern American coastal region using data of December 1990.

The Digisondes/2/ specify the electron density profile by a set of parameters/3,4/ for each ionospheric layer:

$$f_s, f_m, z_m, A_0, A_1, A_2, A_3, A_4 \tag{2}$$

and three of such sets determine the profiles for the E, the F1 and the F2 layers through the relation:

$$z = z_m + \sqrt{g} \sum_{i=0}^{4} A_i T_i^*(g) \tag{3}$$

with:

$$g = \frac{\ln(f/f_m)}{\ln(f_s/f_m)} \tag{4}$$

where z denotes the altitude and f the plasma frequency. T_i^* is the i-th order shifted Chebyshev polynomial/5/. The subscripts s and m denote the values at the starting height and the peak of the layer, respectively. For the F region mapping, we find a new function (3), whenever the F1 layer exists, which describes the profile over the entire F region/6/. This procedure avoids the discontinuity problem, caused by the appearance of F1 at some but not all stations in the mapping region, and causes only minimal distortions.

The general problem is to determine the so-called objective function for the parameter p:

$$p = P(X,Y,t) \tag{5}$$

based on the observed data

$$p_{mn} = P(X_m, Y_m, t_n) \tag{6}$$

$$(m = 1, 2, ..., M;\ n = -N+1, ..., -2, -1, 0)$$

where M specifies the number of stations involved, t_0 denotes the present universal time and N is the number of samples going backward in time. For a given station the data samples form a time series with the interval τ, and the available data base consists of M sets of time series. In our application τ = 30 min, N = 64 and $t_{-N+1} = t_{-63} = t_0 - 31.5h$. By nowcasting we mean calculation of N(X, Y, z, t_0) for the current time t_0, as illustrated later in this paper. The technique also lends itself to short-term forecasting, i.e. for calculation of a 3D map for $t > t_0$. We do not discuss this application here.

The above mathematical presentation of the problem assumes that: (1) at any arbitrary location (X,Y) in the area and at any time t, the electron density profile can be expressed in the same way as at the observation sites; and (2) adequate data density (both spatially and temporally) exists to ensure proper sampling of the main structures and variations in the ionosphere. The first assumption simplifies the problem from finding the electron density profile to finding the function p, equation (5), thus eliminating the variables z. The second assumption limits the

process to spatial variations with wavelengths larger than 2L, and temporal variations larger than 2τ, where τ is the sampling interval and L the average station separation.

2.0 PHYSICAL AND MATHEMATICAL FOUNDATION

Investigations of the ionospheric formation, motion and dependence on solar-terrestrial parameters lead to physical models of the ionosphere. Because of the complicated physical processes involved the theoretical models are generally less accurate than models derived from measured data. Our data drive technique derives from the concept that changes of the ionosphere at any one location relate to those at another location (at least within a limited area), and that ionospheric plasma changes occur in a wave-like form. For example, the diurnal variation at a western location lags in time with respect to a more eastern location. For a morphological description, the time history of the sampled data contains sufficient information to analyze the behavior of the ionospheric changes. The technique decomposes the ionospheric variations in the mapping region into a series of simple plane waves which describe the changing ionosphere at any location. Fourier analysis provides a tool for the wave decomposition and we assume the existence of a Fourier expansion of function (5):

$$P(X,Y,t) = \iiint_{-\infty}^{+\infty} P(\omega,k_x,k_y)\, e^{i(\omega t - k_x X - k_y Y)}\, d\omega\, dk_x\, dk_y \qquad (7)$$

Equation (7) decomposes the time-varying two-dimensional physical field P(X,Y,t) into a series of plane waves. The relation between the spatial wave numbers k_x and k_y and the frequency ω, i.e. the dispersion relation, derives from the dynamic equations of the field and the properties of the medium. We do not intend to study the physical aspects of the field, but simply assume that k_x and k_y are complex functions of ω only, i.e.:

$$k_x = k_x(\omega) + iS_x(\omega)\ ,\ k_y = k_y(\omega) + iS_y(\omega) \qquad (8)$$

This means that the parameters of a wave propagating in a given direction do not depend on location. The objective function becomes:

$$P(X,Y,t) = \int_{-\infty}^{+\infty} P(\omega)\, e^{S_x(\omega)X+S_y(\omega)Y+i[\omega t-k_x(\omega)X-k_y(\omega)Y]}\, d\omega$$

Rewriting $P(\omega)$ as:

$$P(\omega) = A(\omega)\, e^{-i\Phi_0(\omega)} \tag{9}$$

we have:

$$P(X,Y,t) = \int_{-\infty}^{+\infty} A(\omega)\, e^{S_x(\omega)X+S_y(\omega)Y+i[\omega t-k_x(\omega)X-k_y(\omega)Y-\Phi_0(\omega)]}\, d\omega \tag{10}$$

where $A(\omega)$, $S_x(\omega)$, $S_y(\omega)$, $k_x(\omega)$, $k_y(\omega)$ and $\Phi_0(\omega)$ are all real functions.

For any time $t_n \leq t_0$, we calculate the objective function $P(X,Y,t)$ with the help of the discrete Fourier transform (DFT). With $\omega t_n = 2\pi\nu n/N$, $P(X,Y,t_n)$ becomes /7/:

$$P(X,Y,t_n) = \sum_{\nu=-N/2}^{N/2-1} A(\nu) e^{S_x(\nu)X+S_y(\nu)Y-i[k_x(\nu)X+k_y(\nu)Y+\Phi_0(\nu)]+i2\pi n\nu/N} \tag{11}$$

Equation (11) decomposes the time-varying two-dimensional physical field into N damped plane waves with different frequencies and amplitudes. The only important limitation possibly restricting application of (11) resides in equation (8) which assumes that the parameters of any wave in a given direction do not change along the wave trajectory. In this way, the mapping problem reduces to finding the functions $A(\nu)$, $S_x(\nu)$, $S_y(\nu)$, $k_x(\nu)$, $k_y(\nu)$ and $\Phi_0(\nu)$. The next section will show how to resolve the difficulty of phase ambiguity and how to determine these functions.

3.0 DETERMINATION OF THE FOURIER KERNEL

At any station $X=X_m$ and $Y=Y_m$:

$$P(X_m,Y_m,t_n)= \sum_{\nu = -N/2}^{N/2-1} A(\nu)e^{S_xX_m+S_yY_m-i[k_xX_m+k_yY_m+\Phi_0]+i2\pi n\nu/N} \tag{12}$$

We expand the measured data series (6) also into a Fourier series:

$$P(X_m,Y_m,t_n)= \sum_{\nu = -N/2}^{N/2-1} P_m(\nu)e^{i2\pi n\nu/N} \tag{13}$$

Expressing $P_m(\nu)$ in terms of amplitude and phase

$$P_m(\nu) = P_{0m}(\nu)\, e^{-i\Phi_m(\nu)} , \tag{14}$$

$$(-\pi < \Phi_m(\nu) \leq \pi) ,$$

and comparing (12) to (13), we obtain

$$P_{0m}(\nu) = A(\nu)\, e^{S_xX_m+S_yY_m} \tag{15}$$

and

$$\Phi_m(\nu) = k_xX_m+k_yY_m+\Phi_0+2k_m\pi , \tag{16}$$

where $k_m(\nu)$ is an integer, generally 0 or ± 1.

For three stations (M = 3) in the mapping area, equations (15) and (16) determine values of A, S_x, S_y, k_x, k_y and Φ_0 for each ν. For more than three stations, a best-fit technique determines the values.

The error functions

$$\varepsilon_1 = \sum_{m=1}^{M} [\ln P_{0m}(\nu) - \ln A(\nu) - S_x X_m - S_y Y_m]^2 \tag{17}$$

$$\varepsilon_2 = \sum_{m=1}^{M} [\phi_m(\nu) - 2k_m\pi - k_x X_m - k_y Y_m - \phi_0]^2 \tag{18}$$

will be minimized if the $A(\nu)$, S_x, S_y, k_x, k_y and ϕ_0 satisfy the following two sets of relations:

$$\ln A(\nu) M + S_x \sum_{m=1}^{M} X_m + S_y \sum_{m=1}^{M} Y_m = \sum_{m=1}^{M} \ln P_{0m}(\nu)$$

$$\ln A(\nu) \sum_{m=1}^{M} X_m + S_x \sum_{m=1}^{M} X_m^2 + S_y \sum_{m=1}^{M} X_m Y_m = \sum_{m=1}^{M} \ln P_{0m}(\nu) X_m \tag{19}$$

$$\ln A(\nu) \sum_{m=1}^{M} Y_m + S_x \sum_{m=1}^{M} X_m Y_m + S_y \sum_{m=1}^{M} Y_m^2 = \sum_{m=1}^{M} \ln P_{0m}(\nu) Y_m$$

and

$$\phi_0 M + k_x \sum_{m=1}^{M} X_m + k_y \sum_{m=1}^{M} Y_m = \sum_{m=1}^{M} [\phi_m(\nu) - 2k_m\pi]$$

$$\phi_0 \sum_{m=1}^{M} X_m + k_x \sum_{m=1}^{M} X_m^2 + k_y \sum_{m=1}^{M} X_m Y_m = \sum_{m=1}^{M} [\phi_m(\nu) - 2k_m\pi] X_m \tag{20}$$

$$\phi_0 \sum_{m=1}^{M} Y_m + k_x \sum_{m=1}^{M} X_m Y_m + k_y \sum_{m=1}^{M} Y_m^2 = \sum_{m=1}^{M} [\phi_m(\nu) - 2k_m\pi] Y_m$$

These are first-order linear equations. From the first set of equations (19), we find $A(\nu)$, S_x and S_y, and from the second set of equations (20) we find ϕ_0, k_x and k_y.

Consequently, the objective function is determined and the parameter $P(X,Y,t_n)$ is calculated with equation (11) for any location, assuming we can estimate the correct value for the integer k_m in Eq. (20). For the low frequencies, it is expected that the values of Φ_m for different stations are close to each other, so there is no phase ambiguity. For higher frequencies different sets of k_m values ($0_N \pm 1$) are tested as illustrated in the following example. A trial technique, with the least error criteria, generally finds the right values for k_m. Wrong decisions on the k_m values can occur near the Nyquist frequency $1/(2\tau)=1h^{-1}$. Fortunately, these higher spectral components with about 1 hour periods in our analysis correspond to gravity waves that contain little energy and do not introduce serious errors in the resulting maps. The following example illustrates the procedure. The observed phases Φ_m (see Eq. 14) were $\Phi_1 = 12.3°$, $\Phi_2 = 89.8°$, $\Phi_3 = -113.5°$, $\Phi_4 = -170.1°$, $\Phi_5 = -22.4$.

Case #	k_1	k_2	k_3	k_4	k_5	Φ_1	Φ_2	Φ_3	Φ_4	Φ_5
1	0	0	0	0	0	12.3	89.8	-113.5	-170.1	-22.4
2	0	0	0	-1	0	12.3	89.8	-113.5	189.9	-22.4
3	0	0	-1	-1	0	12.3	89.8	246.5	189.9	-22.4
4	0	0	-1	-1	-1	12.3	89.8	246.5	189.9	237.6
5	-1	0	-1	-1	-1	372.3	89.8	246.5	189.9	237.6

A least-squares fitting is done for each case and the one with the best fit is adopted.

4.0 APPLICATION OVER THE NORTHEASTERN AMERICAN COAST

We applied the new technique to mapping the electron density structure over the northeast American coastal region within the area 30° to 60°N and 80° to 50°W. Five Digisonde stations (Figure 1) supplied the data for the regional mapping during December 1990:

Goose Bay, Labrador	(53.32°N, 60.33°W)
Argentia, NF	(47.28°N, 53.97°W)
Millstone Hill, MA	(42.60°N, 72.50°W)
Wallops Island, VA	(37.93°N, 75.47°W)
Bermuda	(32.33°N, 64.67°W)

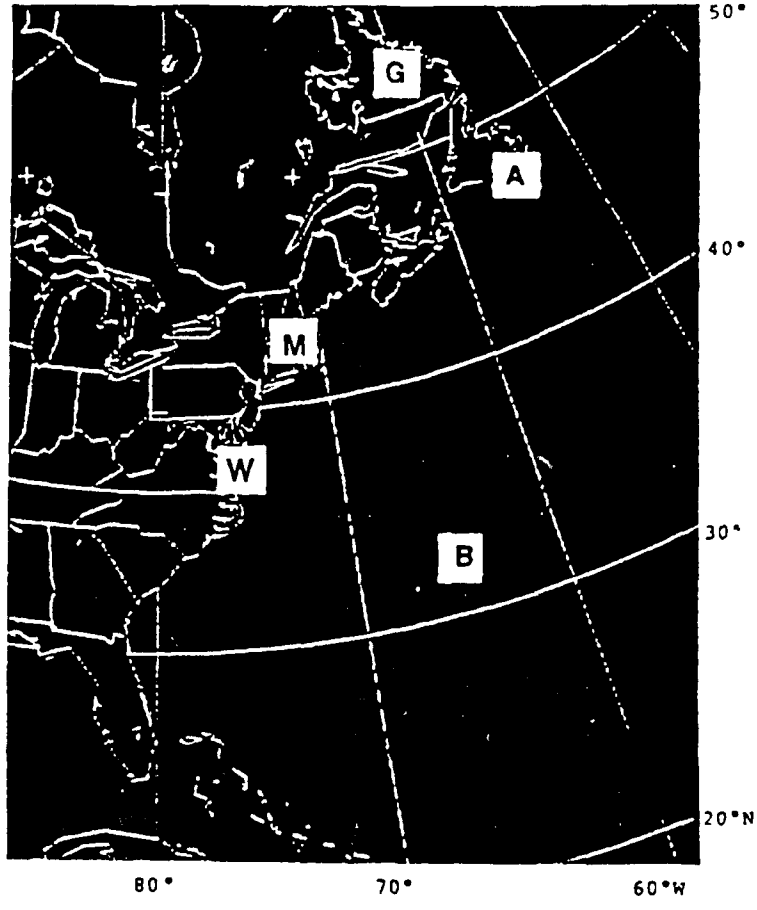

Figure 1. Five Digisonde Stations at the northeast American coastal region (G-Goose Bay, A-Argentia, M-Millstone Hill, W-Wallops Island and B-Bermuda) make routine half-hourly ionograms.

Figure 2 shows the time variations of one of the profile parameters, foF2, for the five stations. Small dots mark the data samples used to calculate the spectrum for 1300 UT on day 349, 1990. For each station a 32 hour time series with 30 minute samples (N=64, τ=30min) was Fourier transformed using an FFT algorithm, resulting in the spectra of Figure 3. The 64 line amplitude spectrum on the left has even symmetry, and the 64 line phase spectrum on the right has odd symmetry as expected for a real function. In the plot a value of 2π had been added to negative phases. The spectral lines represent the values of $P_{0m}(\nu)$ and $\Phi_m(\nu)$, respectively, in equation (14). Figure 3 illustrates the typical behavior of all observed amplitude spectra: a rapid amplitude decrease with frequency. This means that the lower frequencies dominate the three-dimensional profile reconstruction.

Figure 4 illustrates the wave superposition technique displaying the time development of the foF2 parameter in the 30° by 30° mapping region during sunrise, from 1100 UT to 1430 UT. The white dots indicate the locations of the five stations. The gray shade scale on the right side reveals that the plasma frequencies decrease from above 5 MHz in the South-East, to below 4 MHz in the North-West at 1100 UT, and from above 13 MHz to below 11 MHz at 1430 UT. As a consistency check the measured foF2 values at each of the five stations are shown on top of the figure together with the "mapped" value (in parenthesis). For this example of a sunrise period, the differences between measured and mapped values are acceptably small. Figure 4 (on top) also indicates the available data samples for each station. In the current analysis, data gaps were filled by linear interpolations.

Accurate HF ray tracing between two separate points requires the knowledge of the electron distribution in a vertical plane through the two points. This requires the calculation of vertical profiles along the great circle path between the two points. From the objective functions of all parameters specified in (2) the program calculates the two dimensional electron distributions. Figure 5 shows the sequence of east-west profile cross sections through the points (280°, 45°) and (300°, 45°) during sunrise on day 90-349 in half-hour increments. Starting at 1100 UT tilts develop at 305°E longitude which by 1130 UT extend over the entire 2500km region. At 1330 UT the F layer is generally horizontally satisfied, except of a small ondulation.

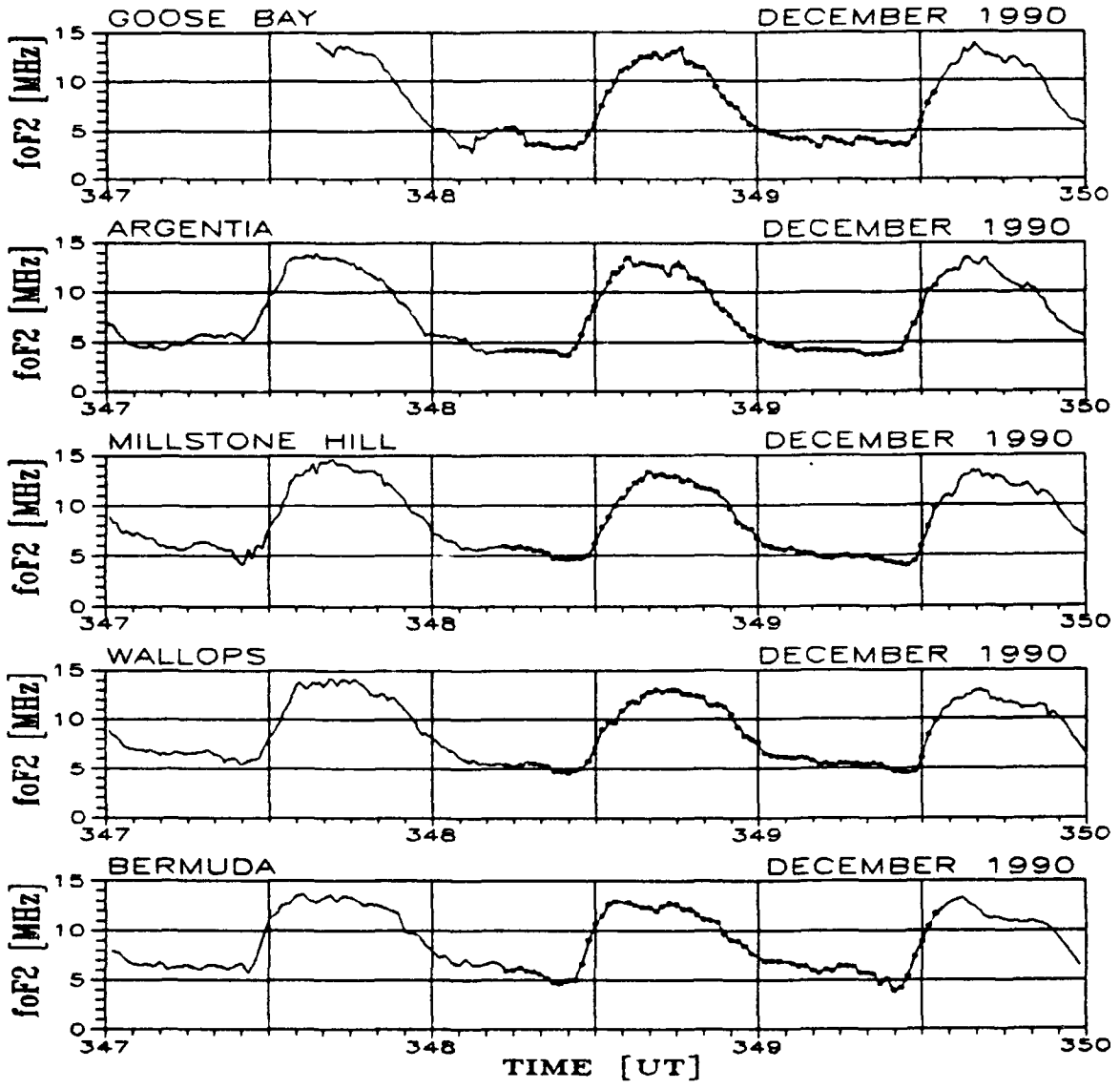

Figure 2. Time-variation of parameter foF2 for 5 stations.

To calculate the contour map for foF2 at 1300 UT on day 349, the previous 32 hours of data for each station are Fourier transformed. The data samples used for constructing the 1300 UT map are marked by small dots.

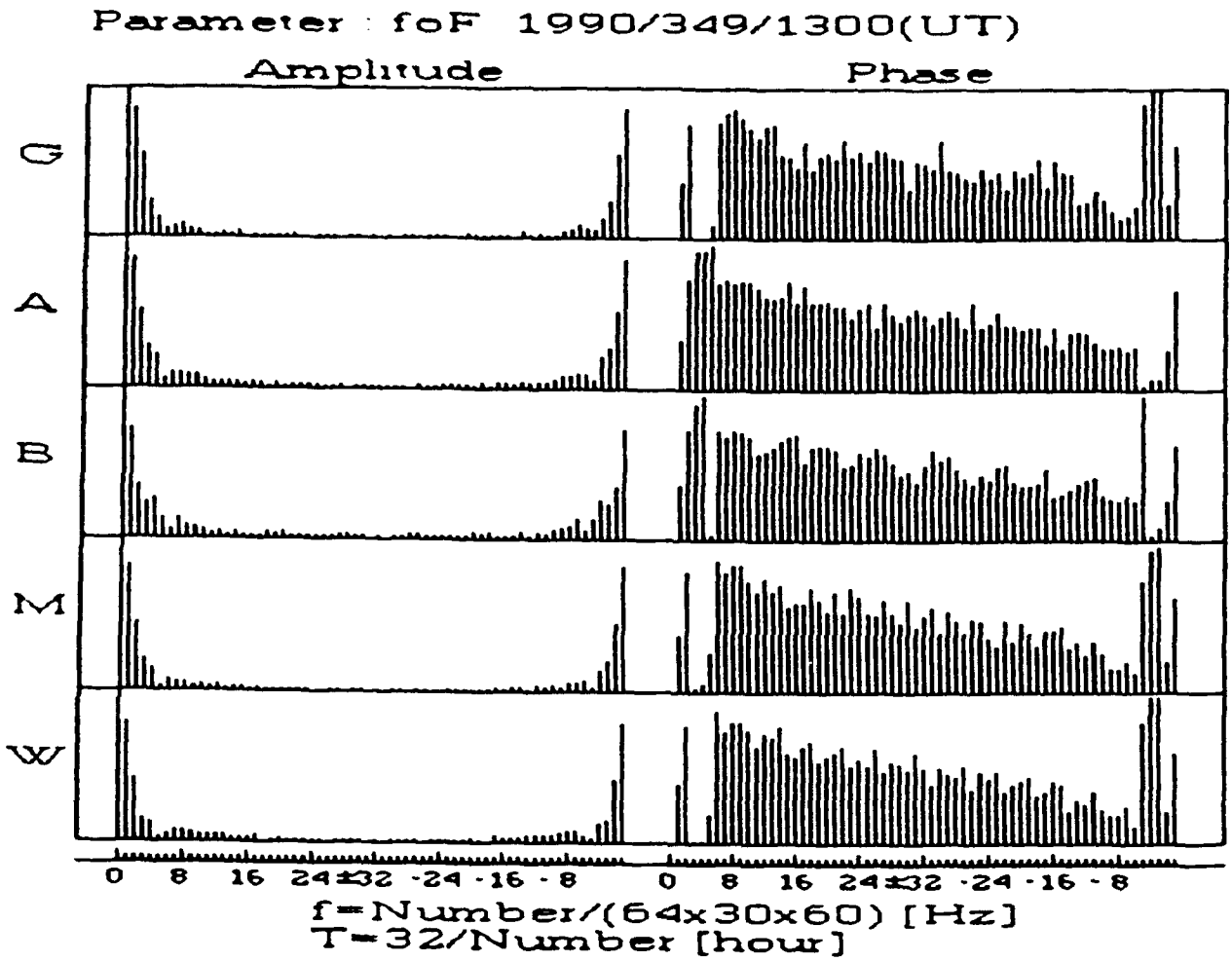

Figure 3 Spectra for parameter foF2 for 5 stations day 349, 1990, 13 UT.

The amplitude spectra determine which "wave frequencies" contribute to the parameter map. The amplitude and phase distribution for each spectrum component over the five stations specifies the attenuation and phase constants and the wave directions. Linear superposition of the set of plane waves generates the parameter contour map for the 30° by 30° area. Once the contour maps for all parameters are specified, the electron density profile at any point in the area is given by equation (3).

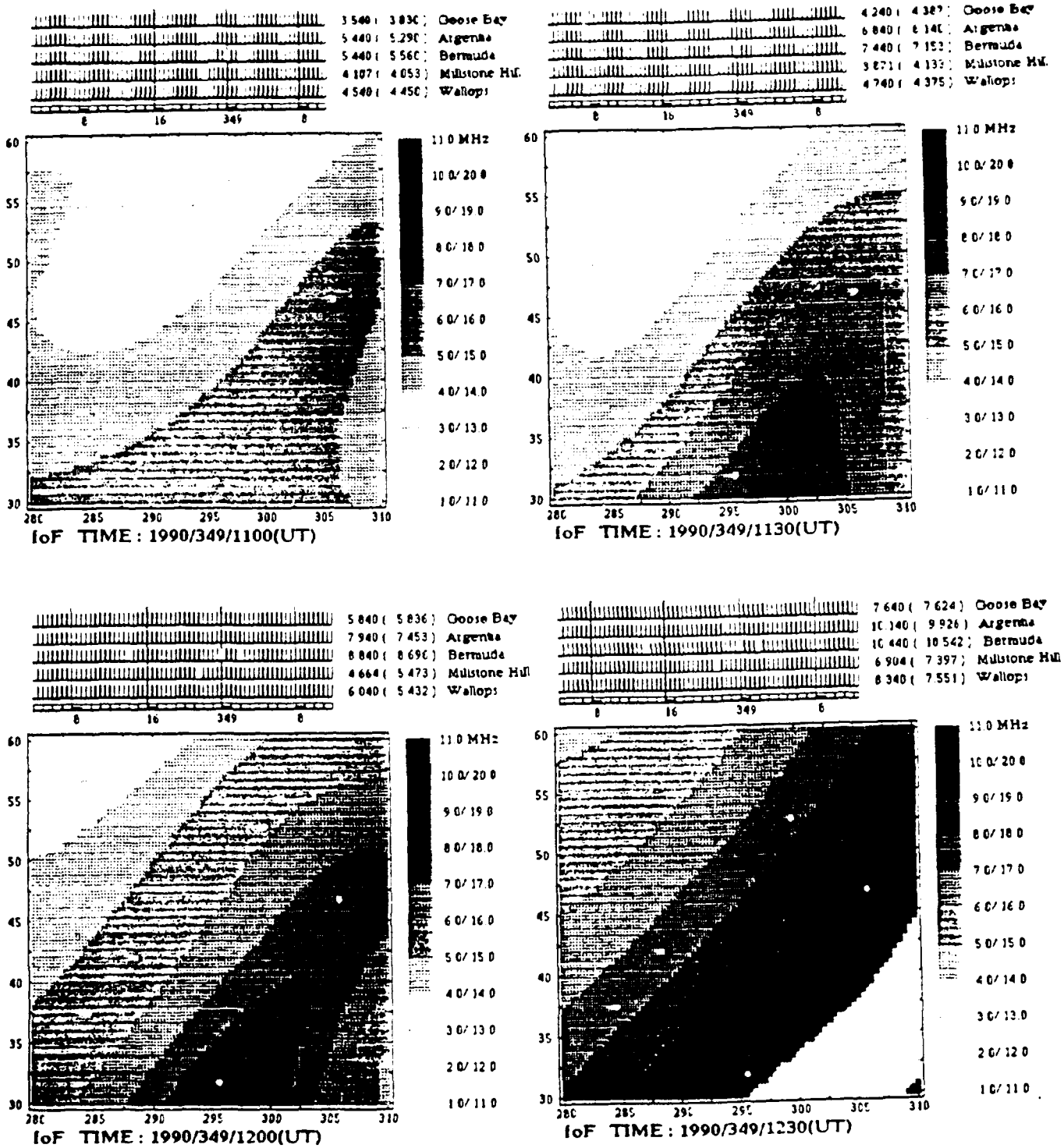

Figure 4. Sunrise sequence of foF2 maps.

Systematic change of the foF2 contours as a function of time; half-hourly increments.

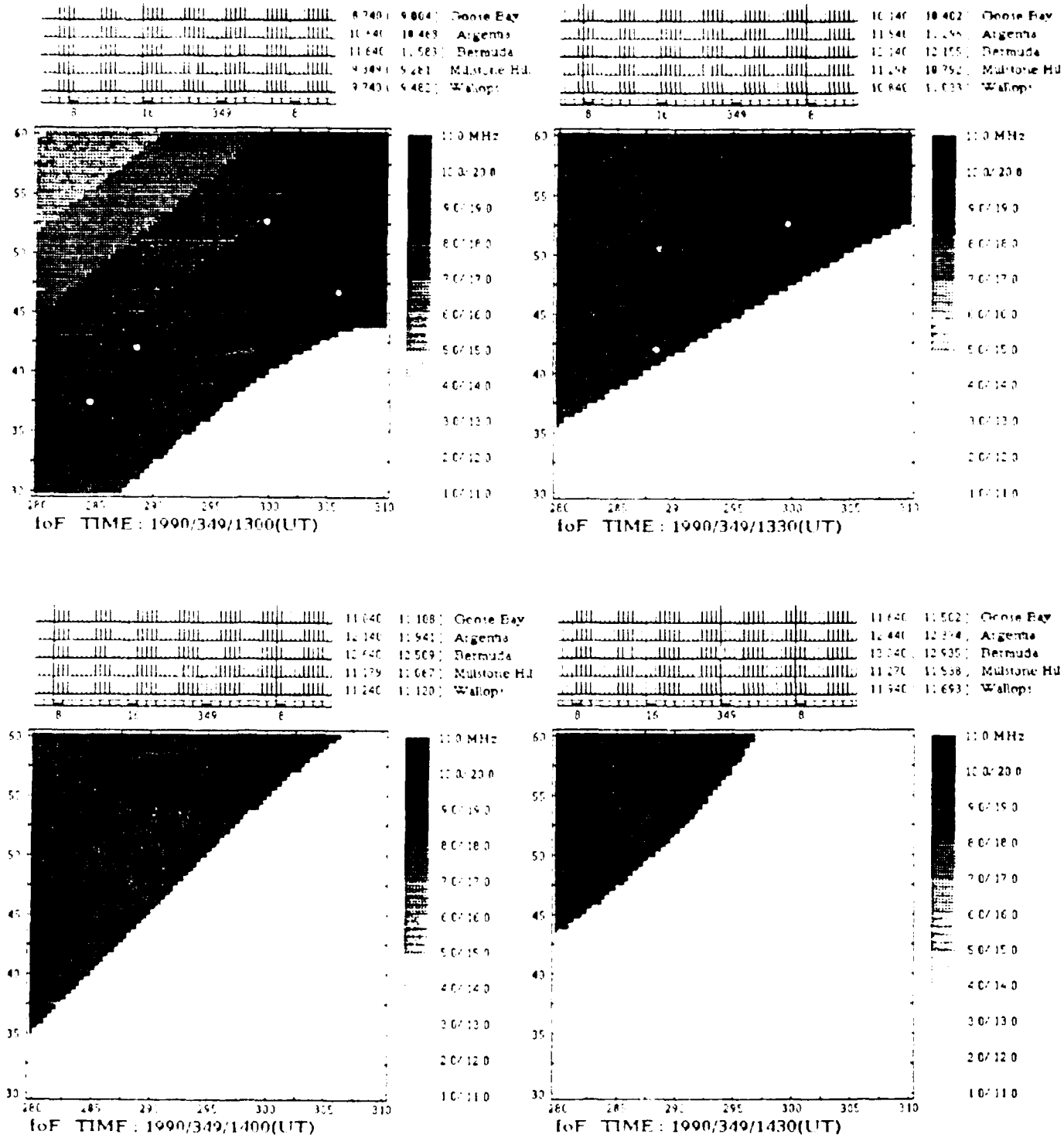

Figure 4. Sunrise sequence of foF2 maps (Concluded)

Systematic change of the foF2 contours as a function of time; half-hourly increments.

The nowcasting software ran on a 386 PC computer in the laboratory. In an operational environment all new data arriving from the stations can feed real-time calculations for continuous generation of updated maps. This method of nowcasting can support OTH radar operation as well as HF communications and direction finding applications. The updated electron density maps will "follow" the changes of the ionosphere. Furthermore, using the measured time series of the parameters from the monitoring stations, this mapping technique can be expanded to forecast near future maps of electron density distribution.

5.0 EVALUATION OF THE NOWCASTING TECHNIQUE

Evaluation of the nowcasting technique requires additional sounding stations located within the mapping area, sufficiently separated from the given monitoring stations. Data from one ionosonde in Maine showed excellent agreement with mapped values, but the distance to the Millstone Hill, MA sounder, which is one of the network sounders, measures only 600 km.

To generate a broad testing database, we used the IRI model/8/ to provide time sequences of profiles for the locations of the five Digisondes and for 16 other locations in the mapping area. The nowcasting algorithm used the profiles from the five sounder locations to calculate the profiles for each of these other locations. Averaging the differences between the database and mapped values over a 24 hour period provides a good measure of the performance of the nowcasting technique.

Figure 6 shows the rms errors in foF2 and hmF2 for the months of January and July, both for sunspot values of R=10 and R=150. The errors remain small within the mapping region, and even in the boundary regions the errors do not grow excessively.

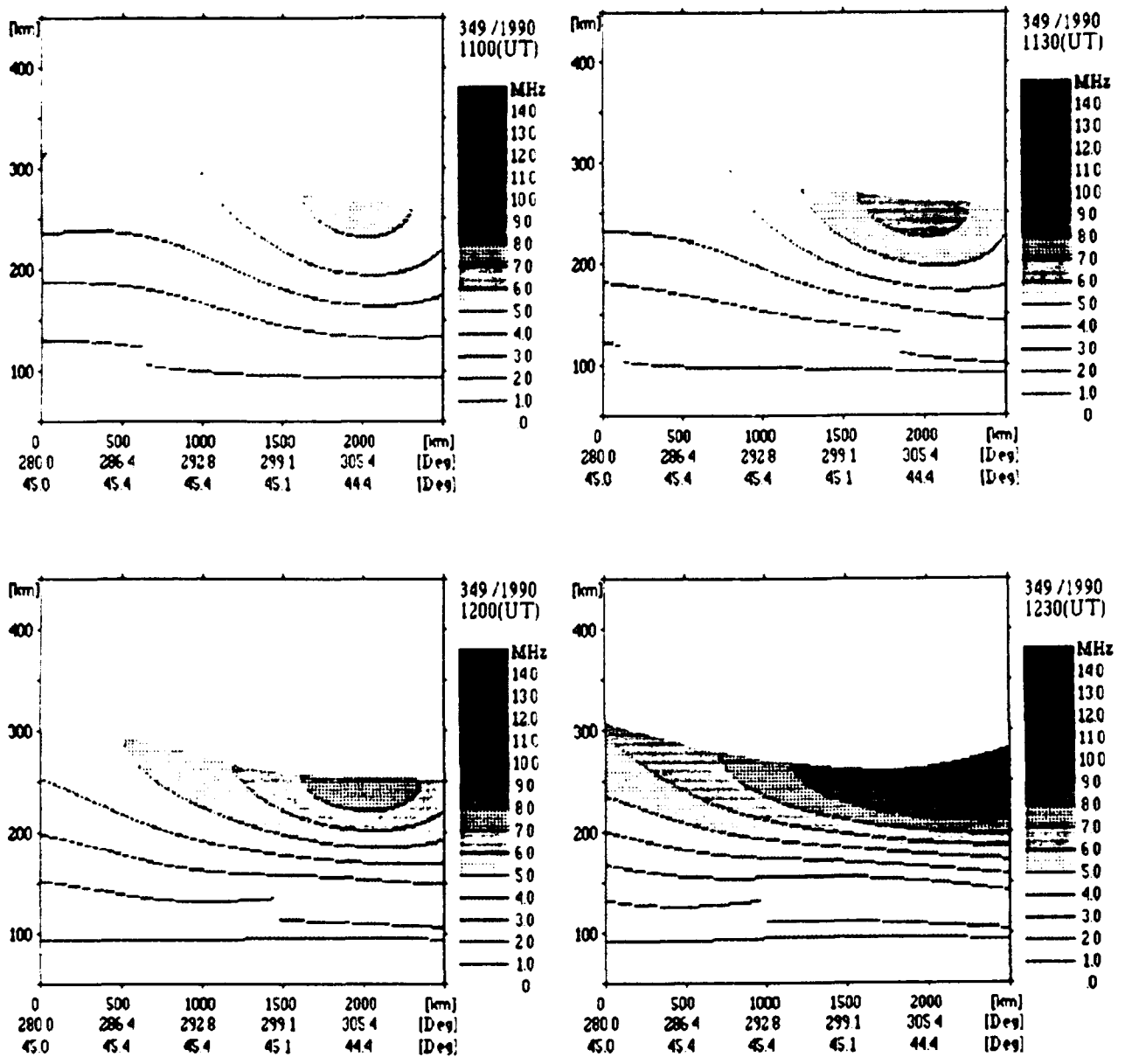

Figure 5. Sunrise sequence of profile cross sections.

Profile cross sections in any direction can be calculated through the mapped area. The time sequence of the east-west cross section during sunrise on day 349 in half-hour increments is shown.

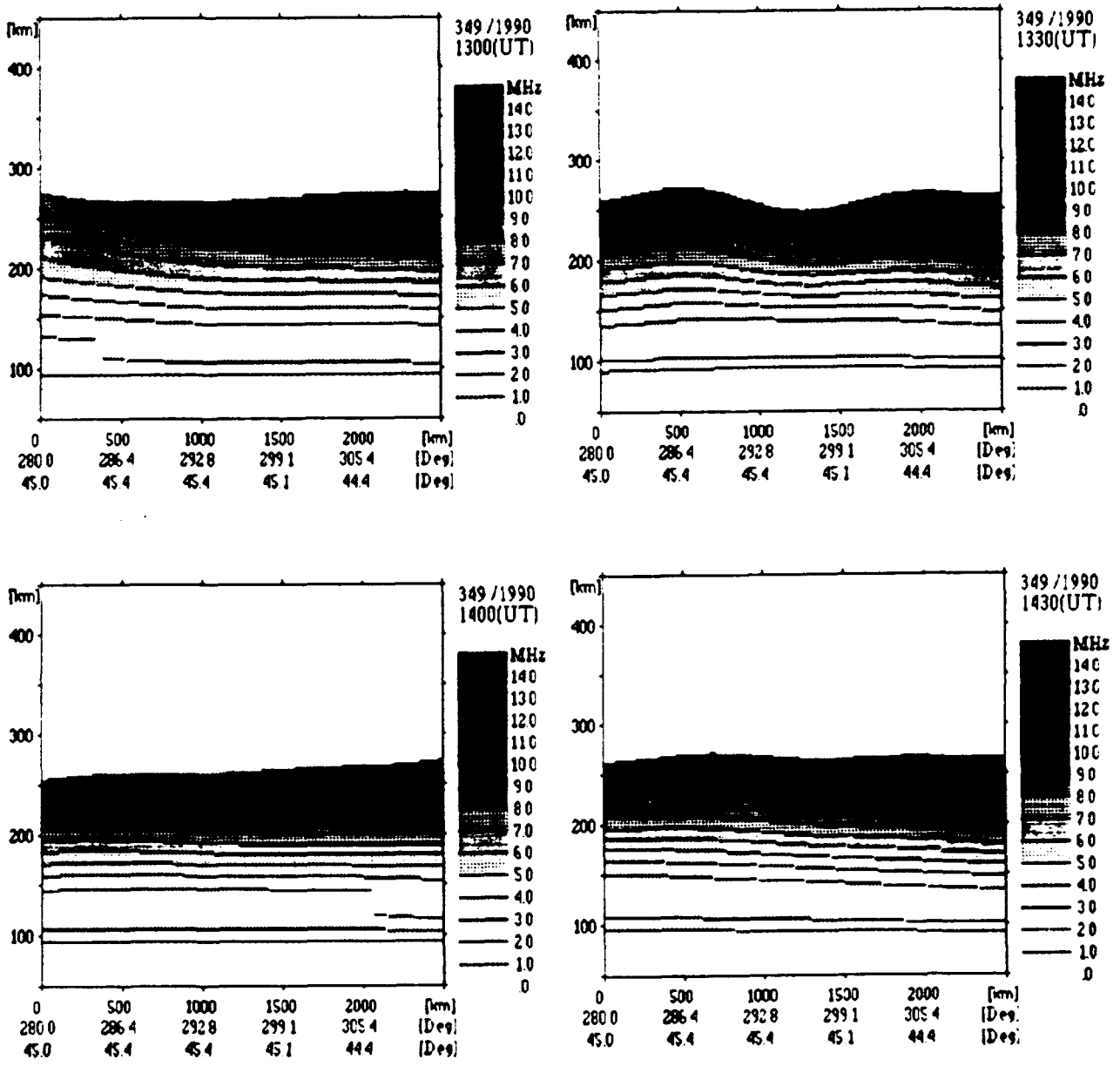

Figure 5. Sunrise sequence of profile cross sections (Concluded).

Profile cross sections in any direction can be calculated through the mapped area. The time sequence of the east-west cross section during sunrise on day 349 in half-hour increments is shown.

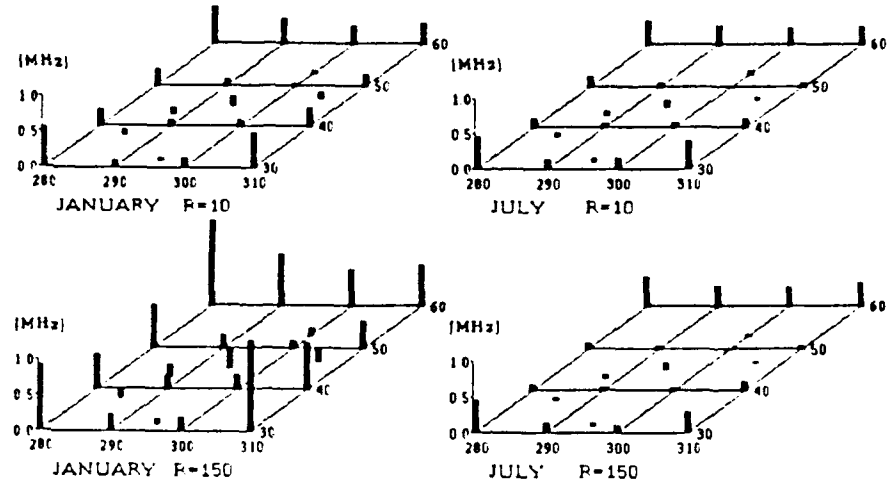

RMS Errors for foF2 Using IRI Data

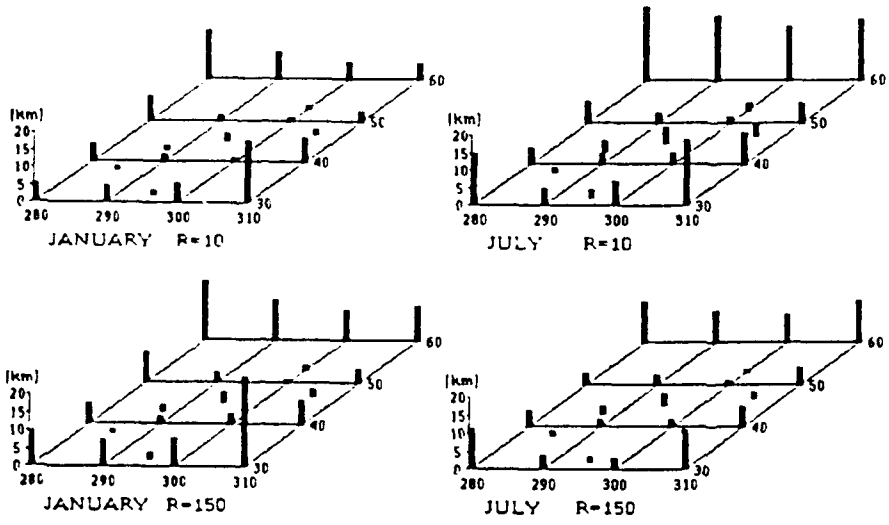

RMS Errors for hmF2 Using IRI Data

Figure 6. Evaluation of the mapping technique using the IRI database. RMS errors for foF2 and hmF2 at the 5 sounder sites and 16 other locations for January and July under low (R=10) and high (R=150) solar activity, respectively.

6.0 SUMMARY

The new data drive mapping technique determines the three dimensional electron density distribution of the ionosphere over a wide area at any time from the time series of observed sounder data. The technique uses the following approach:

1. Characterize electron density profiles by parameter sets, $\{f_s, f_m, z_m, A_0, A_1, A_2, A_3, A_4\}$.

2. Take DFT for each parameter at each station to determine the wave frequencies that contribute to the observed electron density distribution.

3. Determine the best fit plane wave for each frequency from the amplitudes and phases at the five stations.

4. Construct parameter (e.g. f_m) contour map by linear superposition of plane waves.

5. Calculate electron density at area point X,Y using parameters f_s, f_m, z_m, A_0, A_1, A_2, A_3, A_4, specified for this point by the constructed parameter maps.

Preliminary testing over the Northeast American region shows the promise of this technique in support of OTH radar, HF communications and direction finding applications. The potential features of the technique include the capability of providing maps in real time for nowcasting and to make near-term forecasts.

Since the technique is completely data driven, difficulties arise when data gaps in the order of hours or more occur at any monitoring station. This problem requires further studies.

7.0 REFERENCES

1. Reinisch, B.W., R.R. Gamache and L.G. Bossy, "Ionospheric Characteristics for IRI in Real Time," Adv. Space Res., 10, 8, pp. (8)25-(8)34, 1990.

2. Reinisch, B.W., K. Bibl, D.F. Kitrosser, G.S. Sales, J.S. Tang, Z.M. Zhang, T.W. Bullett, and J.A. Ralls, "The Digisonde 256 Ionospheric Sounder," World Ionosphere/Thermosphere Study, WITS Handbook, Vol. 2, Ed. by C.H. Liu, December 1989.

3. Huang, X. and B.W. Reinisch, "Automatic Calculation of Electron Density Profiles from Digital Ionograms. 2. True Height Inversion of Topside Ionograms with the Profile-Fitting Method," Radio Science, 17, 4, pp. 837-844, 1982.

4. Reinisch, B.W. and X. Huang, "Automatic Calculation of Electron Density Profiles from Digital Ionograms. 3. Processing of Bottomside Ionograms," Radio Sci. 18, 477, 1983.

5. Synder, M.A., "Chebyshev Methods in Numerical Approximation," Prentice-Hall, Inc., 1966.

6. Huang, X. and B.W. Reinisch, "Processing of Ionogram Profiles," to be submitted to Radio Science, 1992.

7. Bracewell, R.N., "The Fourier Transformation and its Applications," McGraw-Hill Book Company, 2nd Edition, 1986.

8. Rawer, K. and D. Bilitza, "International Reference Ionosphere - Plasma Densities: Status 1988," Adv. Space Res,. 10, No. 8, 1990.